

Magnetic and transport properties of the spin-state disordered oxide



Soichiro Shibusaki and Ichiro Terasaki*

Department of Applied Physics, Waseda University, Tokyo 169-8555, Japan

Eiji Nishibori and Hiroshi Sawa

Department of Applied Physics, Nagoya University, Nagoya 464-8603, Japan

Jenni Lybeck, Hisao Yamauchi, and Maarit Karppinen

Department of Chemistry, Aalto University School of Science and Technology, FI-00076 Aalto, Finland

We report measurements and analysis of magnetization, resistivity and thermopower of polycrystalline samples of the perovskite-type Co/Rh oxide $\text{La}_{0.8}\text{Sr}_{0.2}\text{Co}_{1-x}\text{Rh}_x\text{O}_{3-\delta}$. This system constitutes a solid solution for a full range of x , in which the crystal structure changes from rhombohedral to orthorhombic symmetry with increasing Rh content x . The magnetization data reveal that the magnetic ground state immediately changes upon Rh substitution from ferromagnetic to paramagnetic with increasing x near 0.25, which is close to the structural phase boundary. We find that one substituted Rh ion diminishes the saturation moment by $9 \mu_B$, which implies that one Rh^{3+} ion makes a few magnetic Co^{3+} ions nonmagnetic (the low-spin state), and causes disorder in the spin state and the highest occupied orbital. In this disordered composition ($0.05 \leq x \leq 0.75$), we find that the thermopower is anomalously enhanced below 50 K. In particular, the thermopower of $x=0.5$ is larger by a factor of 10 than those of $x=0$ and 1, and the temperature coefficient reaches $4 \mu\text{V}/\text{K}^2$ which is as large as that of heavy-fermion materials such as CeRu_2Si_2 .

PACS numbers: 75.30.Cr, 75.30.Wx, 72.15.Jf

I. INTRODUCTION

Cobalt oxides are interesting materials. First, the trivalent cobalt ion in perovskite-related oxides takes different spin states depending on temperature,^{1,2} pressure,^{3,4} structure,⁵ and magnetic field.⁶ Second, hole-doping drives a spin-state crossover to make Co^{3+} ions adopt the intermediate or high-spin state, and causes various magnetic phases.⁷⁻¹⁴ A doped Co^{4+} ion dresses a cloud of magnetic Co^{3+} ions, as observed by neutron scattering.¹⁵ The double exchange mechanism between the low-spin Co^{4+} (t_{2g}^5) and the intermediate-spin Co^{3+} ($e_g^1 t_{2g}^5$) stabilizes an itinerant ferromagnetic state in $\text{La}_{1-x}\text{Sr}_x\text{CoO}_3$, and causes spin glass or cluster glass behavior depending on the Sr concentration.⁹ Third, since the discovery of good thermoelectric properties in the layered cobalt oxide Na_xCoO_2 ,¹⁶ various cobalt oxides have been extensively investigated as possible candidates for oxide thermoelectric materials.¹⁷⁻²² The origin of the large thermopower in the layered cobalt oxides is discussed from viewpoints of band calculation^{23,24} and spin and orbital degeneracy.²⁵

Although Rh is located just below Co in the periodic table, rhodium oxides have been less investigated than their cobalt-oxide counterparts, but recently have attracted considerable attention as candidates for thermoelectric oxides.²⁶⁻³³ An advantage for the thermoelectric application is that the low-spin state is highly stable in Rh^{3+} , which gives a large thermopower in the perovskite rhodium oxides. LaCoO_3 -based oxides show fairly good thermoelectric properties at room temperature,^{34,35} but

the thermopower suddenly decreases to a few $\mu\text{V}/\text{K}$ above 500 K, accompanied by a spin-state crossover.³⁶⁻³⁸ In contrast, LaRhO_3 -based oxides are found to exhibit a large thermopower up to 800 K,^{39,40} which is theoretically explained by Usui *et al.*⁴¹

Comparing the transport properties between $\text{La}_{1-x}\text{Sr}_x\text{CoO}_3$ and $\text{La}_{1-x}\text{Sr}_x\text{RhO}_3$,^{14,38-40,42} we find three differences as follows; (i) For the same doping level, the resistivity of doped LaCoO_3 is one order of magnitude smaller than that of doped LaRhO_3 . (ii) The metal-insulator transition occurs around $x_c = 0.3$ in $\text{La}_{1-x}\text{Sr}_x\text{CoO}_3$; in $\text{La}_{1-x}\text{Sr}_x\text{RhO}_3$, x_c is significantly smaller (~ 0.15). (iii) $\text{La}_{1-x}\text{Sr}_x\text{CoO}_3$ is a ferromagnetic metal, while $\text{La}_{1-x}\text{Sr}_x\text{RhO}_3$ is a Curie-Weiss metal. These three differences are basically ascribed to the difference in the highest occupied orbital of Co/Rh ions. In the doped LaCoO_3 , holes in the e_g orbital are responsible for the conduction, and interact with the Co^{3+} ions through the double exchange mechanism. In the doped LaRhO_3 , in contrast, holes in the t_{2g} orbital are responsible for the conduction. It is thus tempting to study the physical properties of a solid solution of doped LaCoO_3 and LaRhO_3 , where the highest-occupied orbitals and the spin states are disordered. Very recently, Li *et al.*⁴³ reported the structural and thermoelectric properties of $\text{LaCo}_{1-x}\text{Rh}_x\text{O}_3$. We expect that more exotic effects will emerge in the solid-solution system of Co and Rh, when carriers are doped. In this paper, we show the magnetic and transport properties of polycrystalline samples of $\text{La}_{0.8}\text{Sr}_{0.2}\text{Co}_{1-x}\text{Rh}_x\text{O}_{3-\delta}$.

II. EXPERIMENTAL

Polycrystalline samples of $\text{La}_{0.8}\text{Sr}_{0.2}\text{Co}_{1-x}\text{Rh}_x\text{O}_{3-\delta}$ were prepared by a solid-state reaction. The Sr content of 0.2 was chosen based on the fact that the solubility limit of Sr in $\text{La}_{1-y}\text{Sr}_y\text{RhO}_3$ is at $y=0.2$.⁴⁰ At this doping level, $\text{La}_{0.8}\text{Sr}_{0.2}\text{CoO}_3$ is a ferromagnetic semiconductor, and $\text{La}_{0.8}\text{Sr}_{0.2}\text{RhO}_3$ is a Curie-Weiss metal. Thus we expect to observe a systematic evolution between the two states with increasing Rh content x . Stoichiometric amounts of La_2O_3 , SrCO_3 , Co_3O_4 and Rh_2O_3 were mixed and calcined at 1373 K for 24 h in air. The calcined products were thoroughly ground, pelletized and sintered at 1473 K for 48 h in air.

X-ray diffraction patterns were measured using $\text{MoK}\alpha$ radiation (RIGAKU ultraX18 with multilayer mirror) and a Debye-Scherrer camera of radius 286.48 mm with an imaging plate. Oxygen contents of the samples were determined by thermogravimetric H_2 -reduction analysis with reproducibility better than ± 0.03 for $3 - \delta$.⁴⁴ The resistivity was measured using a conventional four-probe technique in a liquid He cryostat from 4.2 to 300 K. The thermopower was measured using a steady-state technique with a typical temperature gradient of 0.5-1 K/cm in a liquid He cryostat from 4.2 to 300 K. Using Magnetic Property Measurement System (MPMS, Quantum Design), the magnetization measurements were performed with an external field of 0.1 T from 5 to 400 K, and the magnetization-field curve was measured from 0 to 7 T at 5 K.

III. RESULTS AND DISCUSSION

From the thermogravimetric reduction experiments, it was revealed that the $\text{La}_{0.8}\text{Sr}_{0.2}\text{Co}_{1-x}\text{Rh}_x\text{O}_{3-\delta}$ system is apparently oxygen-deficient. This is rather common for ambient-pressure-synthesized ACoO_3 -type perovskites based on A-site cations with a lower than +3 valence state in average. For the present samples, the $3 - \delta$ value was determined at 2.95(4), with no evident dependency on x . Consequently we may conclude that in $\text{La}_{0.8}\text{Sr}_{0.2}\text{Co}_{1-x}\text{Rh}_x\text{O}_{3-\delta}$ the average valence of the B-site cations (Co and Rh) remains essentially constant at ca. +3.1 through the whole substitution range, being significantly lower than the value (+3.2) calculated assuming $\delta=0$.

Figure 1(a) shows a typical x-ray diffraction pattern for $x=0.5$. At room temperature, $\text{La}_{0.8}\text{Sr}_{0.2}\text{CoO}_{3-\delta}$ crystallizes in rhombohedral (space group $R\bar{3}c$), $\text{La}_{0.8}\text{Sr}_{0.2}\text{RhO}_{3-\delta}$ in orthorhombic (space group $Pnma$) structure, as is revealed from the evolution of the main peak with x in the inset of Fig. 1(a). Clearly the phase boundary is between $x=0.2$ and 0.25 at room temperature. The lattice parameters of these materials are shown in Fig. 1(b). The lattice parameters increase with increasing Rh content, which is consistent with the larger ionic radius of Rh^{3+} compared to that of Co^{3+} .

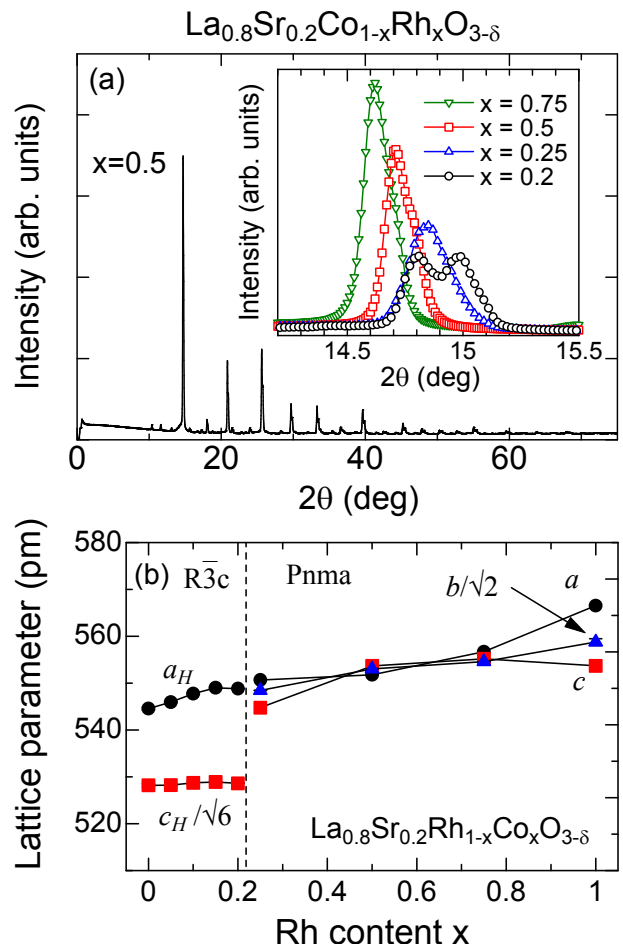


FIG. 1. (Color online) (a) A typical x-ray diffraction pattern and (b) the lattice parameters of $\text{La}_{0.8}\text{Sr}_{0.2}\text{Co}_{1-x}\text{Rh}_x\text{O}_{3-\delta}$. The crystal structure is rhombohedral for $x \leq 0.2$ and orthorhombic for $x \geq 0.25$. The inset shows the x dependence of the main peak near $2\theta = 15$ deg.

This means that the substitution works well, and the Co and Rh species are distributed homogeneously to form a solid solution.

Figure 2 shows the temperature dependence of the magnetization of $\text{La}_{0.8}\text{Sr}_{0.2}\text{Co}_{1-x}\text{Rh}_x\text{O}_{3-\delta}$. A ferromagnetic transition is observed for $\text{La}_{0.8}\text{Sr}_{0.2}\text{CoO}_{3-\delta}$ at around 220 K, as is already reported in literature¹³. The transition temperature and the saturation moment rapidly decrease with increasing Rh content. This means that the substituted Rh ions seriously disrupt the magnetic order. The inverse magnetization is plotted as a function of temperature in Fig. 2(b). The Curie temperature (T_C) is estimated by the extrapolation of the high temperature data as shown by the dotted lines. T_C disappears near $x=0.25$, which coincides with the structural phase boundary shown in Fig. 1(b). The inverse magnetization shows finite values for $0.1 \leq x \leq 0.25$, which indicates that the ferromagnetism within this composition range is not homogeneous, and only a part of the

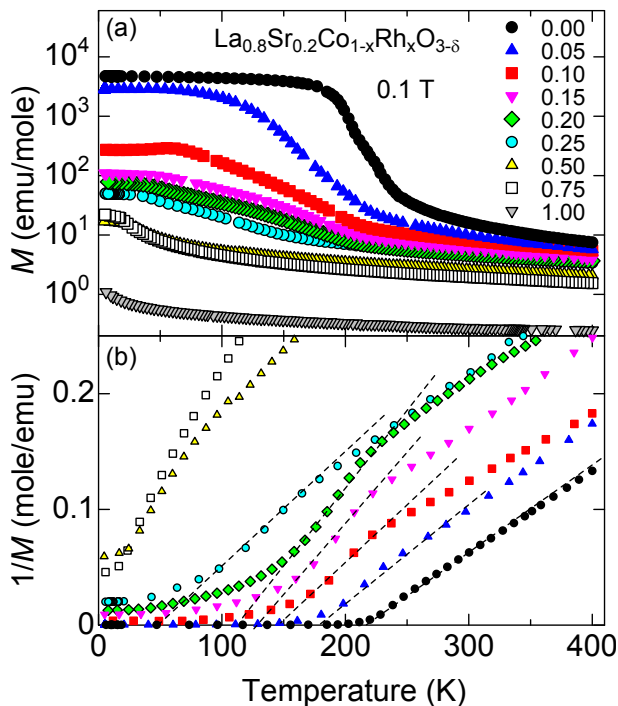


FIG. 2. (Color online) (a) Magnetization M and (b) inverse magnetization $1/M$ of $\text{La}_{0.8}\text{Sr}_{0.2}\text{Co}_{1-x}\text{Rh}_x\text{O}_{3-\delta}$. The dotted lines are guide to the eyes, and indicates the Curie temperature at $1/M=0$.

volume goes ferromagnetic. On the contrary, the inverse magnetization for $x=0.5$ and 0.75 has a positive offset, indicating an antiferromagnetic interaction. The magnetization of $x=1$ shows a value one order of magnitude smaller than that of $x=0.75$, which is consistent with the fact that the Rh^{3+} ions are stable in the low-spin state. However, the magnetization increases with decreasing temperature. Nakamura *et al.*⁴² first measured the susceptibility of this compound, and analyzed the data with a sum of a Curie-Weiss term and a constant term. This suggests that the Rh^{4+} ion does not act as a simple itinerant hole, but works partially as a localized moment. Such a duality of itinerancy and localization is observed in the misfit-layered cobalt oxides.⁴⁵

To discuss the spin states of the present compound, we will briefly review the discussion on the spin states of undoped and doped LaCoO_3 here. As is well known, the spin states of the Co^{3+} ion have been debated for more than forty years, because the low and high-spin states of Co^{3+} are almost degenerate in energy. First of all, there is a consensus that the Co^{3+} ion in LaCoO_3 takes the low-spin state below 10 K, which was suggested by early susceptibility measurement⁴⁶ and was verified by neutron experiment.⁴⁷ Above around 90 K, LaCoO_3 becomes magnetic, which implies that the high-spin or intermediate-spin state is thermally excited above that temperature. Goodenough⁴⁸ originally thought that the high-spin state of Co^{3+} was thermally created. Later

Potze *et al.*⁴⁹ suggested a possibility of the intermediate spin state by introducing the hybridization to the oxygen $2p$ state. Asai *et al.*⁵⁰ reported that there were two magnetic transitions, one near 90 K and a second near 500 K. They further proposed that the lower transition is a crossover from low-spin to the intermediate-spin state.²

The concept of the intermediate-spin state is highly controversial. On the basis of a localized picture, the intermediate-spin state has much higher energy than the low-spin and high-spin states.⁵¹ It is convenient to introduce a concept of ‘ p -hole’ in the presence of hybridization between the transition-metal $3d$ and O $2p$ states.⁵² Using this concept, the intermediate-spin state of Co^{3+} is expressed as a composite of the high-spin state of Co^{2+} ($e_g^2 t_{2g}^5$) antiferromagnetically coupled with one p -hole. Korotin *et al.*⁵³ pointed out that the one e_g electron on the intermediate-spin state of Co^{3+} has an orbital degrees of freedom, and suggested a possibility of orbital ordering as an origin of the nonmetallic nature of LaCoO_3 . Maris *et al.*⁵⁴ observed a monoclinic distortion in LaCoO_3 , which they attributed to a piece of evidence for the orbital ordering. Very recently, Nakao *et al.*⁵⁵ observed $\sigma \rightarrow \pi'$ resonant x-ray scattering in the related cobalt oxide $\text{Sr}_3\text{YCo}_4\text{O}_{10.5}$, which is clear evidence of the orbital ordering of e_g electrons and the existence of the intermediate-spin state as well. On the contrary, some researchers questioned the existence of the intermediate-spin state. Haverkort *et al.*⁵¹ clarified that the spin state of LaCoO_3 is well understood by a mixture of the low-spin and high-spin states from the $\text{Co-L}_{2,3}$ x-ray absorption spectra. They further pointed out that the spectra carried a large orbital moment, which is seriously incompatible with the intermediate-spin state. A similar orbital contribution was detected by electron spin resonance (ESR). From high-field ESR measurement, Noguchi *et al.*⁵⁶ found the g -factor to be 3.35 for LaCoO_3 at 50 K. This value is substantially larger than 2, strongly suggesting the existence of the orbital moment ($L = 1$), and equivalently, the existence of the high-spin state.

The second transition near 500 K is also controversial. At this temperature, LaCoO_3 experiences a metal-insulator transition, and the metallic nature at high temperature is not well understood at present. Heikes *et al.*⁵⁷ claimed that pair formation of Co^{2+} and Co^{4+} should be taken into account for the high-temperature metallic conduction, but this idea was rejected by Jonker.⁴⁶ Raccah and Goodenough¹ proposed a spin-state order, above which the high-spin and low-spin state Co^{3+} ions were ordered in the NaCl-type pattern. However, this ordering was not detected in the neutron experiments.⁵⁸ Asai *et al.*² associated this transition with a crossover from low temperature intermediate-spin to high-temperature high-spin state. Tokura *et al.*¹¹ proposed that this metal-insulator transition can be regarded as a Mott transition where one e_g electron per Co in the intermediate-spin state is identical to a half-filled state. Kobayashi *et al.*⁵⁹ found a similarity in the high-temperature metallic state

between LaCoO_3 and $\text{Sr}_3\text{YCo}_4\text{O}_{10.5}$. In the latter compound, low metallic resistivity is realized above 600 K, together with a small thermopower and Hall coefficient. This indicates that most of the Co^{3+} ions become “itinerant” to make a large Fermi surface in the charge sector. We should note that this metallic state is quite anomalous in the sense that it accompanies a large effective moment of $3.4 \mu_B$ per Co in the spin sector.

Compared with the diverging discussion on LaCoO_3 , the situation is better for the spin state of the doped LaCoO_3 . In this case, the doped hole hops from one Co to another through the hybridization to the oxygen $2p$ state, and the intermediate-spin state can be stabilized relative to the high-spin state.¹⁵ It is now established that the ground state changes from non-magnetic insulator for LaCoO_3 to ferromagnetic metal for $\text{La}_{1-x}\text{Sr}_x\text{CoO}_3$ ($x > 0.25$).^{7–14} Since the magnetic and transport properties of the ferromagnetic $\text{La}_{1-x}\text{Sr}_x\text{CoO}_3$ are similar to those of $\text{La}_{1-x}\text{Sr}_x\text{MnO}_3$, it is natural to associate them with the double exchange mechanism.⁶⁰ For this mechanism, a hole in the e_g band is responsible between the intermediate-spin state of Co^{3+} ($e_g^1 t_{2g}^5$) and the low-spin state of Co^{4+} ($e_g^0 t_{2g}^5$), whereas a hole in the t_{2g} band is responsible between the high-spin state of Co^{3+} ($e_g^2 t_{2g}^4$) and the low-spin state of Co^{4+} (t_{2g}^5). Since the reduction of the kinetic energy of the hole is essential to the double exchange mechanism, the former case is more likely to be realized, because the e_g band is wider than the t_{2g} band. Kriener et al.¹³ showed that the saturation magnetization for ferromagnetic $\text{La}_{0.75}\text{M}_{0.25}\text{CoO}_3$ ($M=\text{Sr}$ and Ba) was $1.65 \mu_B$, which is consistent with the intermediate-spin state of Co^{3+} and the low-spin state of Co^{4+} . Podlesnyak et al.¹⁵ revealed that a spin cluster of one low-spin state Co^{4+} ion surrounded with six intermediate-spin state Co^{3+} ions was localized at low temperature in $\text{La}_{0.998}\text{Sr}_{0.002}\text{CoO}_3$. However, things are not simple; Wu and Leighton⁶¹ claimed that the glassy ferromagnetism of $\text{La}_{1-x}\text{Sr}_x\text{CoO}_3$ is understood by a combination of the intermediate-spin state of Co^{3+} and the *intermediate-spin* state of Co^{4+} . Kriener et al.¹³ also pointed out that the saturation magnetization for $\text{La}_{0.75}\text{Ca}_{0.25}\text{CoO}_3$ is $1 \mu_B$, which is significantly smaller than the Sr-doped sample. As mentioned above, in spite of some controversy, many experiments suggest that Co^{3+} in the doped LaCoO_3 is in the intermediate-spin state. Thus we will assume that the Co^{3+} ions are in the intermediate-spin state in $\text{La}_{0.8}\text{Sr}_{0.2}\text{Co}_{1-x}\text{Rh}_x\text{O}_{3-\delta}$.

Figure 3 shows the magnetization-field ($M-H$) curves of $\text{La}_{0.8}\text{Sr}_{0.2}\text{Co}_{1-x}\text{Rh}_x\text{O}_{3-\delta}$ at 5 K. The magnetic moment of $\text{La}_{0.8}\text{Sr}_{0.2}\text{CoO}_{3-\delta}$ at 7 T is $1.55 \mu_B$, which is well understood by the combination of the intermediate-spin state for Co^{3+} ($S = 1$) and the low-spin state of Co^{4+} ($S = 1/2$). For $x = 0.05$, the hysteresis loop broadens possibly because the substituted Rh acts as a strong pinning center. Looking at the magnetization at 7 T, we find that the saturation magnetization decreases by $0.45 \mu_B$ from $x=0$ to 0.05, which implies that one Rh ion decreases the magnetic moment by $9 \mu_B$. Assuming

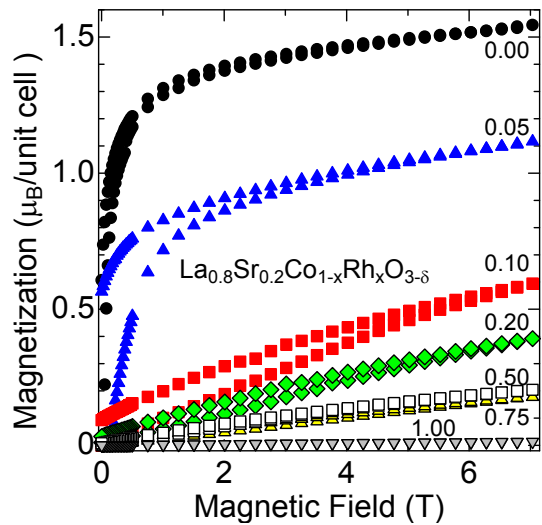


FIG. 3. (Color online) Magnetization-field curves for $\text{La}_{0.8}\text{Sr}_{0.2}\text{Co}_{1-x}\text{Rh}_x\text{O}_{3-\delta}$ at 5 K.

the intermediate-spin state for Co^{3+} ($2 \mu_B$), we estimate that three to four Co^{3+} ions transfer to the low-spin state per one substituted Rh ion. For $x = 0.1$, the $M-H$ curves are almost linear with a tiny hysteresis, suggesting a tiny fraction of the ferromagnetic order. From $x=0.05$ to 0.1, the saturation magnetization decreases by $0.5 \mu_B$, which is close to the rate from $x=0$ to 0.05. As a result, the spin state of the Co^{3+} ions is disordered in $\text{La}_{0.8}\text{Sr}_{0.2}\text{Co}_{1-x}\text{Rh}_x\text{O}_{3-\delta}$, as the intermediate-spin Co^{3+} is partially converted to the low-spin state by the substituted Rh ions. Concomitantly, disorder is induced in the highest-occupied orbitals of t_{2g} and e_g . We notice that the magnetization does not saturate, but continues to increase above 4 T with almost the same slope from $x=0$ to 0.1, although we do not understand the origin for this. For $x > 0.1$, the magnetization is almost linear in external field, the slope decreasing with x .

Next let us focus on the transport properties. Figure 4(a) shows the temperature dependence of the resistivity of $\text{La}_{0.8}\text{Sr}_{0.2}\text{Co}_{1-x}\text{Rh}_x\text{O}_{3-\delta}$. The values for $x=0$ and 1 are consistent with those given in literature,^{38,40} and the values for the intermediate compositions increase monotonically with increasing Rh content x at 300 K. This indicates that the room-temperature resistivity is roughly understood as an average of the two end phases. We should note that the resistivity of the $x=0$ sample exhibits an upturn below 100 K, which is ascribed to the electronic phase separation of the spin clusters.^{61,62} The spin cluster consisting of the low-spin Co^{4+} surrounded with the intermediate-spin Co^{3+} cloud can move rather freely at room temperature, and is gradually confined by the low-spin Co^{3+} ions in the background with decreasing temperature. Thus, although the room-temperature resistivity is less than $1 \text{ m}\Omega\text{cm}$, the carriers are eventually localized at low temperatures. In contrast, the resistivity for $x=1$ shows a metallic conduction down to

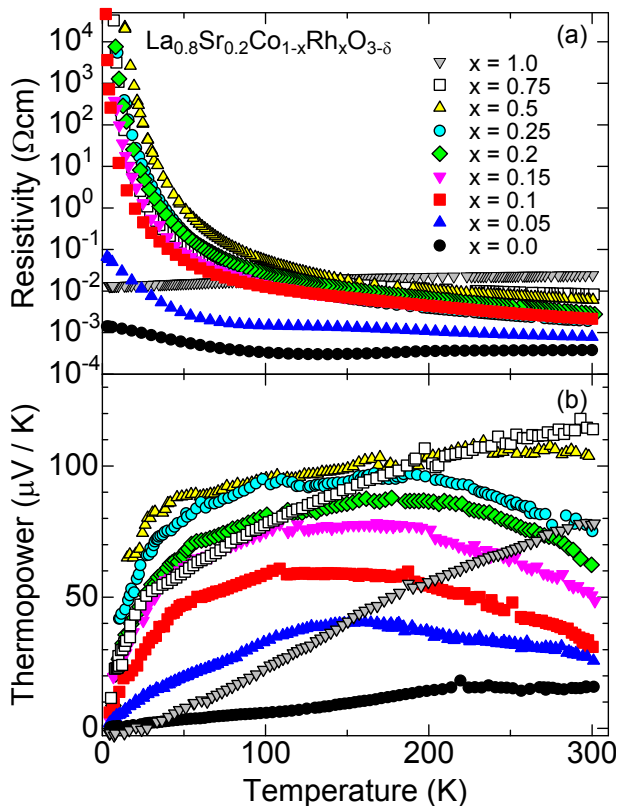


FIG. 4. (Color online) (a) Resistivity and (b) thermopower for $\text{La}_{0.8}\text{Sr}_{0.2}\text{Co}_{1-x}\text{Rh}_x\text{O}_{3-\delta}$.

4 K with a large value of the order of 10 m Ωcm , owing to the narrow t_{2g} band. The effect of the solid solution is drastic at low temperatures. The $x=0.05$ sample shows a strong localization below 50 K, which suggests that the substituted Rh works as a strong pinning center. As was discussed above, one substituted Rh creates a few nonmagnetic Co^{3+} ions at 5 K, which can disrupt the motion of the spin cluster. For $x > 0.10$, the resistivity shows non-metallic temperature dependence at all temperatures, which is explained by the variable-range-hopping transport. This implies that the conduction paths are seriously disordered owing to the disorder in the highest occupied orbital. A similar resistivity is seen in the layered oxide Bi-Ba-(Co,Rh)-O.⁶³

Figure 4(b) shows the temperature dependence of the thermopower of $\text{La}_{0.8}\text{Sr}_{0.2}\text{Co}_{1-x}\text{Rh}_x\text{O}_{3-\delta}$, in which the data for the two end phases are consistent with those given in literature.^{38,40} The thermopower for $x=0$ is small and roughly linear in temperature, indicating a metallic nature of this composition. A small cusp is seen near 220 K, which is close to the Curie temperature. On the other hand, the data for $x=1$ show a large value of 80 $\mu\text{V}/\text{K}$ at room temperature, which suggests that the band effective mass is substantially large owing to the narrow t_{2g} bands. The temperature dependence is roughly linear in temperature, indicating that the electronic states are essentially

understood as a metal. The effects of the solid solution to the thermopower are remarkable. The thermopower is enhanced particularly at low temperatures. For example, the thermopower for $x=0.05$ at 50 K is *larger* than those for $x=0$ and 1, which strongly suggests that the electronic states for $0.05 \leq x \leq 0.75$ cannot be understood from a simple average of $x=0$ and 1. With increasing x from 0.05, the thermopower systematically increases up to 0.5, and exceeds $k_B/e=86 \mu\text{V}/\text{K}$ at 50 K for $x=0.5$, which is ten times larger than those of $x=0$ and 1. We should note that simple disorder cannot enhance the thermopower because this quantity is insensitive to the grain boundary scattering.⁶⁴ We should also note that the oxygen vacancies cannot be the origin of this enhancement either, as our oxygen-content analysis indicated that oxygen content and therefore the carrier density remains essentially constant in $\text{La}_{0.8}\text{Sr}_{0.2}\text{Co}_{1-x}\text{Rh}_x\text{O}_{3-\delta}$. A similar phenomenon is seen in the misfit-layered Rh/Co oxides, but the effect of the solid solution is subtle; the thermopower for $x=0.5$ slightly exceeds those for $x=0$ and 1 near 300 K.⁶³

The temperature dependence of the thermopower for $0.05 \leq x \leq 0.75$ is rather complicated. The thermopower is roughly linear in temperature below about 30 K, nearly independent of temperature from 50 to 200 K. It slowly decreases with increasing temperature above 200 K for $0.05 \leq x \leq 0.25$. The thermopower of $\text{La}_{1-x}\text{Sr}_x\text{CoO}_3$ decreases with increasing temperature above 200 K,³⁸ which is attributed to a precursor of the high-temperature metallic state above 500 K. Since Co is the main B-site constituent for $x \leq 0.25$, the high-temperature electronic states tend to favor those of $\text{La}_{1-x}\text{Sr}_x\text{CoO}_3$. For $x=0.5$ and 0.75, on the other hand, the thermopower continues to increase up to 300 K, which resembles the thermopower of $\text{La}_{1-x}\text{Sr}_x\text{RhO}_3$.⁴⁰

Let us have a closer look at the thermopower at low temperatures. Below 100 K, gross features of the thermopower are similar to those of the layered cobalt and rhodium oxides.^{18–22,26} Limelette *et al.*⁶⁵ have proposed that the low-temperature thermopower of the misfit-layered cobalt oxides can be understood by a sum of a constant term and a T -linear term, corresponding to the spin part and the Fermi liquid part, respectively. Figure 5 shows S/T plotted as a function of $1/T$. For small $1/T$ (i.e. high temperature), S/T is roughly linear in $1/T$, indicating that S is weakly dependent on T . With increasing $1/T$, the behavior starts to deviate from the linear relation as indicated by the arrows, and S/T tends to saturate. In other words, S/T goes towards a constant value for a large $1/T$ (low temperature). In this context, the temperature indicated by the arrows corresponds to the onset temperature of the T -linear thermopower. It should be noted that S/T for $x=0.25$ is anomalously large. It seems to approach $\sim 4 \mu\text{V}/\text{K}^2$ at zero temperature, although S/T still increases in the measured temperature range. Behnia *et al.*⁶⁶ have found a universal relationship between S/T and the electron specific heat

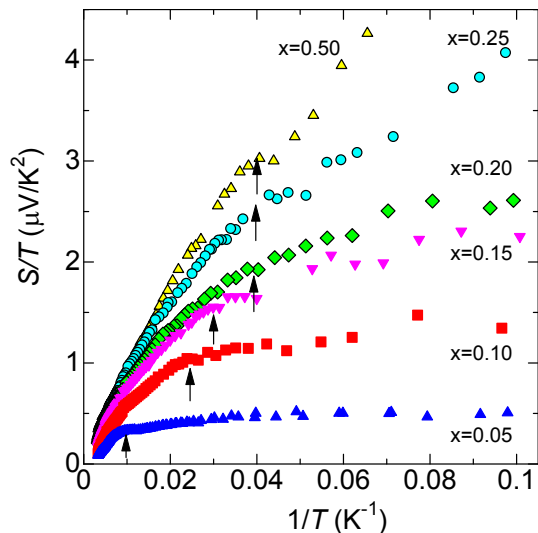


FIG. 5. (Color online) The thermopower divided by temperature S/T plotted as a function of $1/T$. The arrows represent the degenerate temperature below which the thermopower is roughly linear in temperature.

coefficient γ , such that the thermopower is given by

$$S = K_0 \frac{k_B}{e} \frac{T}{T_0}, \quad (1)$$

where T_0 is the degenerate temperature (the Fermi temperature) and K_0 is a constant of the order of unity. Equation (1) implies that T_0 is of the order of $10 - 10^2$ K from $S/T = 4 \mu\text{V}/\text{K}^2$. Since the temperature indicated by the arrows in Fig. 5 is of the same order of T_0 , we identify this temperature to T_0 like heavy fermion and/or mixed valence materials. In fact the value of $S/T = 4 \mu\text{V}/\text{K}^2$ is close to S/T of the heavy-fermion materials, CeRu_2Si_2 and CeCoIn_5 .⁶⁶ However, we notice that the resistivity is highly non-metallic, and the electronic states are even qualitatively different from these materials.

Here we will examine Behia's relationship of S/T to γ for $\text{La}_{1-x}\text{Sr}_x\text{CoO}_3$. The S/T value for $x = 0$ is about $0.1 \mu\text{V}/\text{K}^2$, which corresponds to $\gamma = 10 \text{ mJ}/\text{mol K}^2$. This value is smaller than the observed $30 \text{ mJ}/\text{mol K}^2$ reported by He et al.⁶⁷ This is not surprising, because the ground state of $\text{La}_{1-x}\text{Sr}_x\text{CoO}_3$ is a ferromagnetic metal, not a paramagnetic Fermi liquid. A similar situation is seen in the doped LaMnO_3 ; the thermopower is negligibly small ($\pm 5 \mu\text{V}/\text{K}$ at 77 K),⁶⁸ and γ is $5 \text{ mJ}/\text{mol K}^2$ for the metallic region.⁶⁹ Okuda et al.⁶⁹ pointed out that the Kadowaki-Woods relation is seriously broken down in the doped LaMnO_3 , where the T^2 coefficient of the resistivity is too large to compare with other correlated metals. This indicates that the double-exchange mediated ferromagnetic metals cannot be understood from the conventional Fermi liquid ground state. On the other hand, our sample of $x = 0.5$ is paramagnetic, which can be compared with some heavy fermion compounds.

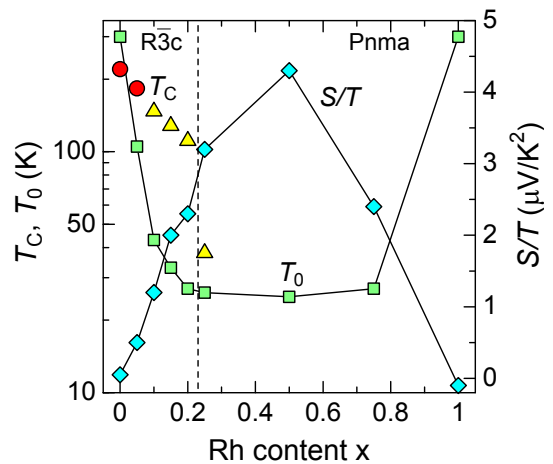


FIG. 6. (Color online) Phase diagram of $\text{La}_{0.8}\text{Sr}_{0.2}\text{Rh}_{1-x}\text{Co}_x\text{O}_{3-\delta}$. T_C and T_0 correspond to the Curie temperature determined in Fig. 3, and the degenerate temperature determined in Fig. 5, respectively. The circles indicate the Curie temperature as a bulk transition, and the triangles represent a kink temperature seen in Fig. 2(b). In the right axis, the temperature coefficient of the thermopower S/T at 15 K is also plotted.

Figure 6 summarizes the electric phase diagram of the title compound, where T_C and T_0 correspond to the Curie temperature determined in Fig. 3 and the degenerate temperature determined in Fig. 5, respectively. Although T_0 for $x=0$ and 1 should be above 300 K, we plot it at 300 K. We plot T_C with different marks, circles and triangles. The circle corresponds to a bulk ferromagnetic transition, i.e., the divergence of the susceptibility in the absence of external field. In Fig. 2(b), $1/M$ for $x = 0$ and 0.05 touches the abscissa axis below T_C . On the other hand, $1/M$ for $x = 0.1, 0.15$ and 0.2 shows a kink at T_C , but remains finite below. This indicates that only a part of the sample goes ferromagnetic, and thus we plot the kink temperature with triangles as a Curie temperature for a partial ferromagnetic order. In the same figure, we plot S/T evaluated at 15 K. As mentioned above, the ferromagnetism appears only in the rhombohedral phase, although the transition is not of bulk nature for $x \geq 0.1$. The degenerate temperature is roughly independent of x from 0.2 to 0.75, and correlates with S/T . This means that the enhancement in S/T is related to neither the ferromagnetism nor the crystal structure, but is related to the disorder induced by the solid solution of Co and Rh.

Finally let us discuss a possible origin for the enhanced S/T for $0.05 \leq x \leq 0.75$. As discussed above, the spin state and the highest occupied orbital are disordered in this solid solution, which induces additional entropy in the system. Since the thermopower reflects entropy per carrier,^{40,70} we expect that the enhanced thermopower found here is related to the entropy due to the disorder in the spin state and/or the highest occupied orbital. In the

perovskite-related oxide $\text{Sr}_3\text{YCo}_4\text{O}_{10.5}$,⁵ partial substitution of Ca for Sr substantially enhances the thermopower, which is associated with the spin state crossover of the Co^{3+} ions. In the same oxide, also partial substitution of Rh for Co enhances the thermopower.⁷⁰ These two examples indicate that the spin state distribution of the Co^{3+} ions affects the thermopower, and we think that a similar mechanism works in the present system as well. Further experimental and theoretical studies are of course necessary to examine this conjecture.

IV. SUMMARY

We have presented the transport and magnetic properties of the perovskite-type Co/Rh oxide $\text{La}_{0.8}\text{Sr}_{0.2}\text{Co}_{1-x}\text{Rh}_x\text{O}_{3-\delta}$. From the magnetization-field curve, we find that one substituted Rh ion makes 3-4 Co^{3+} ions transfer to the low-spin state at 5 K, and causes disorder in the spin state. As a result, the ferromagnetic order in $x=0$ immediately vanishes at $x = 0.10$, while a part of the sample remains ferromagnetic near the crystal structure phase boundary at $x = 0.25$. While the resistivity systematically changes with x at 300 K,

it is highly non-metallic for $0.05 \leq x \leq 0.75$ at low temperatures. This suggests that the spin state disorder acts as a strong pinning center. The most remarkable effect is that the thermopower is anomalously enhanced for $0.05 \leq x \leq 0.75$. In particular, the thermopower for $x=0.5$ exceeds k_B/e at 50 K, which is ten times as large as those for $x=0$ and 1. The enhanced thermopower looks similar to the thermopower of heavy fermion or mixed valence materials, but the origin of the enhancement should be different. We suggest that disorder in the spin state or the highest-occupied orbital is the origin for the additional entropy that attaches the conduction electrons to enhance the thermopower.

ACKNOWLEDGMENTS

The authors would like to thank Y. Klein, M. Abdel-Jawad, and T. Tynell for fruitful discussion. K. Noguchi is thanked for sample preparation at an early stage of this study. This work was partially supported by a Grant-in-Aid for Scientific Research, MEXT (No. 21340106), Japan and by Strategic Japanese-Finland Cooperative Program on “Functional Materials”, JST, Japan, and Academy of Finland (No. 130352).

-
- * Email me at: terra@cc.nagoya-u.ac.jp ; Present address: Department of Physics, Nagoya University, Nagoya 464-8602, Japan
- ¹ P. M. Raccach and J. B. Goodenough, *Phys. Rev.* **155**, 932 (1967).
 - ² K. Asai, A. Yoneda, O. Yokokura, J. M. Tranquada, G. Shirane, and K. Kohn, *J. Phys. Soc. Jpn.* **67**, 290 (1998).
 - ³ T. Vogt, J. A. Hriljac, N. C. Hyatt, and P. Woodward, *Phys. Rev. B* **67**, 140401 (2003).
 - ⁴ J. Baier, S. Jodlauk, M. Kriener, A. Reichl, C. Zobel, H. Kierspel, A. Freimuth, and T. Lorenz, *Phys. Rev. B* **71**, 014443 (2005).
 - ⁵ S. Yoshida, W. Kobayashi, T. Nakano, I. Terasaki, K. Matsubayashi, Y. Uwatoko, I. Grigoraviciute, M. Karppinen, and H. Yamauchi, *J. Phys. Soc. Jpn.* **78**, 094711 (2009).
 - ⁶ S. Kimura, Y. Maeda, T. Kashiwagi, H. Yamaguchi, M. Hagiwara, S. Yoshida, I. Terasaki, and K. Kindo, *Phys. Rev. B* **78**, 180403 (2008).
 - ⁷ G. Jonker and J. V. Santen, *Physica* **19**, 120 (1953).
 - ⁸ V. G. Bhide, D. S. Rajoria, C. N. R. Rao, G. R. Rao, and V. G. Jadhao, *Phys. Rev. B* **12**, 2832 (1975).
 - ⁹ M. Itoh, I. Natori, S. Kubota, and K. Motoya, *J. Phys. Soc. Jpn.* **63**, 1486 (1994).
 - ¹⁰ S. Yamaguchi, Y. Okimoto, H. Taniguchi, and Y. Tokura, *Phys. Rev. B* **53**, R2926 (1996).
 - ¹¹ Y. Tokura, Y. Okimoto, S. Yamaguchi, H. Taniguchi, T. Kimura, and H. Takagi, *Phys. Rev. B* **58**, R1699 (1998).
 - ¹² H. Masuda, T. Fujita, T. Miyashita, M. Soda, Y. Yasui, Y. Kobayashi, and M. Sato, *J. Phys. Soc. Jpn.* **72**, 873 (2003).
 - ¹³ M. Kriener, C. Zobel, A. Reichl, J. Baier, M. Cwikel, K. Berggold, H. Kierspel, O. Zabara, A. Freimuth, and T. Lorenz, *Phys. Rev. B* **69**, 094417 (2004).
 - ¹⁴ K. Berggold, M. Kriener, C. Zobel, A. Reichl, M. Reuther, R. Müller, A. Freimuth, and T. Lorenz, *Phys. Rev. B* **72**, 155116 (2005).
 - ¹⁵ A. Podlesnyak, M. Russina, A. Furrer, A. Alfonsov, E. Vavilova, V. Kataev, B. Büchner, T. Strässle, E. Pomjakushina, K. Conder, and D. I. Khomskii, *Phys. Rev. Lett.* **101**, 247603 (2008).
 - ¹⁶ I. Terasaki, Y. Sasago, and K. Uchinokura, *Phys. Rev. B* **56**, R12685 (1997).
 - ¹⁷ R. Funahashi, I. Matsubara, H. Ikuta, T. Takeuchi, U. Mizutani, and S. Sodeoka, *Jpn. J. Appl. Phys.* **39**, L1127 (2000).
 - ¹⁸ A. C. Masset, C. Michel, A. Maignan, M. Hervieu, O. Toulemonde, F. Studer, B. Raveau, and J. Hejtmanek, *Phys. Rev. B* **62**, 166 (2000).
 - ¹⁹ Y. Miyazaki, K. Kudo, M. Akoshima, Y. Ono, Y. Koike, and T. Kajitani, *Jpn. J. Appl. Phys.* **39**, L531 (2000).
 - ²⁰ T. Itoh and I. Terasaki, *Jpn. J. Appl. Phys. Part 1* **39**, 6658 (2000).
 - ²¹ A. Maignan, L. B. Wang, S. Hébert, D. Pelloquin, and B. Raveau, *Chem. Mater.* **14**, 1231 (2002).
 - ²² S. Hébert, D. Flahaut, C. Martin, S. Lemonnier, J. Noudem, C. Goupil, A. Maignan, and J. Hejtmanek, *Prog. Solid State Chem.* **35**, 457 (2007).
 - ²³ D. J. Singh, *Phys. Rev. B* **61**, 13397 (2000).
 - ²⁴ K. Kuroki and R. Arita, *J. Phys. Soc. Jpn.* **76**, 083707 (2007).
 - ²⁵ W. Koshibae, K. Tsutsui, and S. Maekawa, *Phys. Rev. B* **62**, 6869 (2000).
 - ²⁶ S. Okada and I. Terasaki, *Jpn. J. Appl. Phys.* **44**, 1834 (2005).

- ²⁷ S. Okada, I. Terasaki, H. Okabe, and M. Matoba, *J. Phys. Soc. Jpn.* **74**, 1525 (2005).
- ²⁸ Y. Klein, S. Hébert, D. Pelloquin, V. Hardy, and A. Maignan, *Phys. Rev. B* **73**, 165121 (2006).
- ²⁹ Y. Okamoto, M. Nohara, F. Sakai, and H. Takagi, *J. Phys. Soc. Jpn.* **75**, 023704 (2006).
- ³⁰ S. Shibusaki, W. Kobayashi, and I. Terasaki, *Phys. Rev. B* **74**, 235110 (2006).
- ³¹ W. Kobayashi, S. Hébert, D. Pelloquin, O. Pérez, and A. Maignan, *Phys. Rev. B* **76**, 245102 (2007).
- ³² A. Maignan, V. Eyert, C. Martin, S. Kremer, R. Frésard, and D. Pelloquin, *Phys. Rev. B* **80**, 115103 (2009).
- ³³ S. Shibusaki, T. Nakano, I. Terasaki, K. Yubuta, and T. Kajitani, *J. Phys.: Condensed Matter* **22**, 115603 (2010).
- ³⁴ P. Migiakis, J. Androulakis, and J. Giapintzakis, *J. Appl. Phys.* **94**, 7616 (2003).
- ³⁵ J. Androulakis, P. Migiakis, and J. Giapintzakis, *Appl. Phys. Lett.* **84**, 1099 (2004).
- ³⁶ R. Robert, M. Aguirre, P. Hug, A. Reller, and A. Weidenkaff, *Acta Materialia* **55**, 4965 (2007).
- ³⁷ R. Robert, M. H. Aguirre, L. Bocher, M. Trottmann, S. Heiroth, T. Lippert, M. Dbeli, and A. Weidenkaff, *Solid State Sciences* **10**, 502 (2008), ISSN 1293-2558, *frontiers in Solid State Chemistry*.
- ³⁸ K. Iwasaki, T. Ito, T. Nagasaki, Y. Arita, M. Yoshino, and T. Matsui, *J. Solid State Chem.* **181**, 3145 (2008).
- ³⁹ S. Shibusaki, Y. Takahashi, and I. Terasaki, *J. Phys.: Condensed Matter* **21**, 115501 (4pp) (2009).
- ⁴⁰ I. Terasaki, S. Shibusaki, S. Yoshida, and W. Kobayashi, *Materials* **3**, 786 (2010).
- ⁴¹ H. Usui, R. Arita, and K. Kuroki, *J. Phys.: Condensed Matter* **21**, 064223 (4pp) (2009).
- ⁴² T. Nakamura, T. Shimura, M. Itoh, and Y. Takeda, *J. Solid State Chem.* **103**, 523 (1993).
- ⁴³ J. Li, A. E. Smith, K.-S. Kwong, C. Powell, A. W. Sleight, and M. Subramanian, *J. Solid State Chem.* **183**, 1388 (2010).
- ⁴⁴ M. Karppinen, M. Matvejeff, K. Salomäki, and H. Yamauchi, *J. Mater. Chem.* **12**, 1761 (2002).
- ⁴⁵ J. Bobroff, S. Hébert, G. Lang, P. Mendels, D. Pelloquin, and A. Maignan, *Phys. Rev. B* **76**, 100407 (2007).
- ⁴⁶ G. H. Jonker, *J. Appl. Phys.* **37**, 1424 (1966).
- ⁴⁷ K. Asai, P. Gehring, H. Chou, and G. Shirane, *Phys. Rev. B* **40**, 10982 (1989).
- ⁴⁸ J. B. Goodenough, *J. Phys. Chem. Solids* **6**, 287 (1958).
- ⁴⁹ R. H. Potze, G. A. Sawatzky, and M. Abbate, *Phys. Rev. B* **51**, 11501 (1995).
- ⁵⁰ K. Asai, O. Yokokura, N. Nishimori, H. Chou, J. M. Tranquada, G. Shirane, S. Higuchi, Y. Okajima, and K. Kohn, *Phys. Rev. B* **50**, 3025 (1994).
- ⁵¹ M. W. Haverkort, Z. Hu, J. C. Cezar, T. Burnus, H. Hartmann, M. Reuther, C. Zobel, T. Lorenz, A. Tanaka, N. B. Brookes, H. H. Hsieh, H. J. Lin, C. T. Chen, and L. H. Tjeng, *Phys. Rev. Lett.* **97**, 176405 (2006).
- ⁵² J. Zaanen, G. A. Sawatzky, and J. W. Allen, *Phys. Rev. Lett.* **55**, 418 (1985).
- ⁵³ M. A. Korotin, S. Y. Ezhov, I. V. Solovyev, V. I. Anisimov, D. I. Khomskii, and G. A. Sawatzky, *Phys. Rev. B* **54**, 5309 (1996).
- ⁵⁴ G. Maris, Y. Ren, V. Volotchaev, C. Zobel, T. Lorenz, and T. T. M. Palstra, *Phys. Rev. B* **67**, 224423 (2003).
- ⁵⁵ H. Nakao, T. Murata, D. Bizen, Y. Murakami, K. Ohoyama, K. Yamada, S. Ishiwata, W. Kobayashi, and I. Terasaki, *J. Phys. Soc. Jpn.* **80**, in press (2011).
- ⁵⁶ S. Noguchi, S. Kawamata, K. Okuda, H. Nojiri, and M. Motokawa, *Phys. Rev. B* **66**, 094404 (2002).
- ⁵⁷ R. Heikes, R. Miller, and R. Mazelsky, *Physica* **30**, 1600 (1964).
- ⁵⁸ G. Thornton, B. C. Tofield, and A. W. Hewat, *J. Solid State Chem.* **61**, 301 (1986).
- ⁵⁹ W. Kobayashi, S. Yoshida, and I. Terasaki, *J. Phys. Soc. Jpn.* **75**, 103702 (2006).
- ⁶⁰ Y. Tokura, A. Urushibara, Y. Moritomo, T. Arima, A. Asamitsu, G. Kido, and N. Furukawa, *J. Phys. Soc. Jpn.* **63**, 3931 (1994).
- ⁶¹ J. Wu and C. Leighton, *Phys. Rev. B* **67**, 174408 (2003).
- ⁶² J. Wu, H. Zheng, J. F. Mitchell, and C. Leighton, *Phys. Rev. B* **73**, 020404 (2006).
- ⁶³ S. Okada, A. Sakai, T. Kanno, S. Yotsuhashi, and H. Adachi, *J. Appl. Phys.* **105**, 083711 (2009).
- ⁶⁴ A. Carrington and J. R. Cooper, *Physica C* **219**, 119 (1994).
- ⁶⁵ P. Limelette, S. Hébert, V. Hardy, R. Frésard, C. Simon, and A. Maignan, *Phys. Rev. Lett.* **97**, 046601 (2006).
- ⁶⁶ K. Behnia, D. Jaccard, and J. Flouquet, *J. Phys.: Condensed Matter* **16**, 5187 (2004).
- ⁶⁷ C. He, S. Eisenberg, C. Jan, H. Zheng, J. F. Mitchell, and C. Leighton, *Phys. Rev. B* **80**, 214411 (2009).
- ⁶⁸ P. Mandal, *Phys. Rev. B* **61**, 14675 (2000).
- ⁶⁹ T. Okuda, Y. Tomioka, A. Asamitsu, and Y. Tokura, *Phys. Rev. B* **61**, 8009 (2000).
- ⁷⁰ I. Terasaki, M. Iwakawa, T. Nakano, A. Tsukuda, and W. Kobayashi, *Dalton Transactions* **39**, 1005 (2010).